Published in final edited form as:
Anal Chem. 2012 March 6; 84(5): 2105–2110. doi:10.1021/ac2032707.

3D Imaging by Mass Spectrometry: A New Frontier

Erin H. Seeley and **Richard M. Caprioli**

Summary

Imaging mass spectrometry can generate three-dimensional volumes showing molecular distributions in an entire organ or animal through registration and stacking of serial tissue sections. Here we review the current state of 3D imaging mass spectrometry as well as provide insights and perspectives on the process of generating 3D mass spectral data along with a discussion of the process necessary to generate a 3D image volume.

Molecular imaging of tissue sections by mass spectrometry (MS) has become an enabling technology in biological and medical research.[1–4] The ability to produce molecular images directly from sections with high mass accuracy brings new and exciting possibilities to significantly advance the knowledge and understanding of health and disease. Thin tissue sections are collected onto a target plate and a laser or ion beam raster of the tissue section inside the mass spectrometer is used to desorb analytes, producing mass spectra at discrete coordinate locations. Any of the thousands of signals that are recorded in the mass spectrum from each spot or pixel can give rise to an image, when the intensity of a signal (peak) is plotted for each pixel in the array. A wide variety of molecules can be imaged in this way including proteins, peptides, lipids, and endogenous and exogenous metabolites. The sample preparation can be optimized based on the class of molecule to be imaged. A detailed description of these analyses has been previously reviewed.[5] Moreover, multiple two dimensional mass spectrometric images can be used to reconstruct a three dimensional map of these molecules throughout the sample structure through the use of image processing software.[6] Early experiments have been shown in 3D IMS using DESI[7] and LAESI[8], however, this discussion will focus on 3D IMS by matrix assisted laser desorption/ionization (MALDI) and secondary ion mass spectrometry (SIMS). Each has unique strengths and applications and these will be discussed in more detail below. Imaging mass spectrometry (IMS) is advantageous in that no prior knowledge of analytes present in the tissue section is necessary and that many hundreds of images can be produced from a single raster of the tissue.

3D Imaging (Depth Profiling) with SIMS

Time-of-flight secondary ion mass spectrometry (TOF-SIMS) has been used for many years to generate molecular images and depth profiles of samples including tissue sections.[9,10] SIMS uses a high energy, high spatial resolution ion beam to bombard the sample surface resulting in the ejection of secondary ions originating from the molecules on the surface that can be measured by mass spectrometry. SIMS sources are typically either liquid metal ion guns (LMIG) such as Ga^+ or In^+ or cluster guns such as Au_3^+ or C_{60}^+. LMIG are higher in energy due to high acceleration potential and small particle size and tend to cause fragmentation of biomolecules limiting the obtainable mass range to <1 kDa. Cluster guns provide softer ionization due to some of the energy being dissipated through breaking up of the cluster as it impacts the surface and can be used for the analysis of intact molecules up to 1–2 kDa. Three dimensional SIMS imaging can be carried out using two different

approaches. In the first, serial sections of a tissue are collected and individual 2D images are collected from the tissue section that can be later reconstructed into a 3D image. The second is a depth profiling approach in which a single biological sample is eroded and imaged generating several layers of mass spectral data throughout a z-stack of the sample. Depth resolution in 3D SIMS changes depending on the nature of the substrate (i.e. density, topography). Concurrent measurements using atomic force microscopy can aid in the determination of the thickness of the layer sampled. Recently, the depth profiling of Langmuir-Blodgett monolayers (a model system that simulates cell membranes) that are comprised of 4.4 nm thick layers of barium dimyristoyl phospahtidate (DMPA) embedded in thick multilayers of barium arachidate has been shown.[11] A C_{60}^+ gun was used to alternately erode a 300–500 μm area and image at a spatial resolution of 1–2 μm. An optimal depth resolution of 12.1 nm was obtained by conducting the imaging experiment at 100 K with a 20 keV C_{60}^+ beam at a 71° incident angle. While the depth resolution was larger than the thickness of the DMPA layer, it could be clearly distinguished from the barium arachidate multilayer (Figure 1). Newer instrumentation allows for depth profiling of samples without the need for alternating imaging and etching.[12] This new approach uses linear bunching of pulses to simultaneously image and erode the surface, allowing reconstruction of these data in a three-dimensional representation of the surface.

SIMS technology has also been used for 3D imaging of HeLa cells.[13] Cells were prepared both by hydrated freeze fracture in a *mousetrap* device and by formalin fixation freeze drying. The cells were imaged using a 40 keV C_{60}^+ cluster beam at 1 μm spatial resolution. A total of 10 layers of mass spectral data were acquired through the cells. The first two layers appeared very similar to each other, but a marked change was observed at the third layer where the nucleus is first encountered. The cell membranes contain a high abundance of an ion at *m/z* 184 that corresponds to the phosphatidylcholine head group of glycerophospholipids. In contrast, the nucleus contains characteristic ions at *m/z* 136 and 152 that correspond to $[M+H]^+$ ions of adenine and guanine, respectively (Figure 2). Overall, the signal intensity was found to be lower in the nuclei of the cells than in the surroundings. The cells prepared by hydrated freeze fracture produced data with higher signal-to-noise ratios. It is suspected that this is due to the presence of water in the sample and therefore an increase abundance of protons that can aid ionization of the analytes within the samples. Data were visualized as individual 2D images showing the distribution of ions in each plane. PCA analysis was carried out in MATLAB to determine at what level the substrate (stainless steel or silicon) was encountered and thus could be used to determine the thickness of each layer. Data were also reconstructed into 3D images using AVS Express to display the three-dimensional distributions of phosphocholine and adenine throughout the cell. Adenine could clearly be observed localized to the nucleus within the cell and phosphocholine was found to surround the nucleus comprising the cellular membrane.

SIMS can also be carried

MALDI Imaging Mass Spectrometry

MALDI utilizes a matrix, typically a small organic crystalline compound in an organic solvent that is applied to the tissue surface to facilitate the extraction, desportion, and ionization of the analytes form the tissue surface.[14–16] MALDI MS technology can be used to analyze a broad range of analytes with the best spatial resolution of approximately 5–20 μm.

Since its introduction in 1997,[17] the technology used for MALDI Imaging Mass Spectrometry (IMS) has rapidly advanced. The first image was acquired manually on a PerSeptive Voyager Elite equipped with a 20 Hz nitrogen laser and required several hours to

acquire and image of a ~1 mm^2 area of a rat pituitary. Custom software was designed for the reconstruction and visualization of the mass spectral image. In 1999, automated acquisition of a MALDI tissue image was reported[18] which greatly reduced the time required for data acquisition. The introduction of solid state lasers, such as the Nd:YAG laser,[19] increased repetition rates (200–1000 Hz) and vastly improved lifetimes. Currently, instrument manufactures are offering software designed for image acquisition and viewing such as Bruker FlexImaging, AB SciEx TissueView, Waters HDImaging, and Thermo ImageQuest. These advances have made tissue imaging more generally useful and available in research laboratories. Recently, higher repetition rate lasers (5 kHz or greater) have been implemented in imaging mass spectrometers that allow the acquisition of images of an intact sagittal section of a rat brain (185 mm^2) in less than 10 minutes.[20]

Most early MALDI IMS studies were focused on the analysis of animal tissue and organs. The rat brain[21–24] has been a popular specimen for the evaluation of new matrix application and mass spectral technologies as the many substructures allow for determination of the degree of delocalization observed and the bilateral symmetry of coronal sections serves to evaluate image homogeneity.

3D Imaging of Brain Structures

An initial report demonstrating 3D MALDI IMS of the mouse brain was published by Crecelius *et al*.[25] in 2005. This specimen was a logical starting place for an initial study due to its small size and the existence of anatomical references that could be used as guides. This report visualized myelin basic protein in a 3D rendered volume of the corpus collosum of a mouse brain. A mouse brain was sectioned coronally at 20 μm thickness resulting in a total of 264 collected sections. Reference points were added to each slide using paper and toner ink to act as fiducials, or alignment points, between the optical images and the mass spectral images. Photographs were taken of each section that were subsequently used to reconstruct the brain volume.

Ten sections, equally spaced through the brain (400–500 μm apart), were selected for mass spectral analysis. Each of these sections were manually coated with sinapinic acid using a TLC sprayer and imaged using an Applied Biosystems MALDI TOF Voyager DE-STR mass spectrometer at 100 μm spatial resolution. Mass spectrometry images were viewed as Analyze 7.5 (*.img) data files, a common file format compatible with many data analysis programs including BioMap (Novartis, Basel, Switzerland) and MATLAB (Mathworks, Natick, MA). Following mass spectral analysis, matrix was removed from the surface of the tissue and the sections were Nissl stained to allow visualization of the corpus collosum within the sections. All 264 optical images were used to construct a 3D volume of the brain using Maya software (Autodesk, Inc.). Interior features (in particular the corpus collosusm) were used as main points for registration. Only x,y positioning and z-rotation were allowed during the registration; no resizing or warping was done. The corpus collosum was then segmented out of the total brain volume using the FastRBF Interpolation Toolbox (Farfield Technology, Inc.).

Mass spectral images corresponding to two isoforms of myelin basic protein were generated for each of the 10 sections and registered to their optical sections through the use of the signal from the fiducial points. The corpus collosum data were then segmented out of the total protein images and were inserted at the appropriated locations into this volume. Through the use of the fiducials for alignment and considering the height difference between paper and tissue, the error in positioning was estimated to be less than the width of a single pixel (100 μm). The results of this reconstruction are shown in Figure 3. This experiment was an important first step in the 3D co-registration of MALDI ion images with other imaging modalities.

In 2008, Andersson *et al.*[26] reported 3D imaging of both peptides and proteins within the substantia-nigra and the interpeduncular nucleus within the rat brain. In this study, serial 12 μm coronal sections were collected on two MALDI target plates, one plate for protein analysis and one for peptide analysis. A spacing of 200 μm was used between collected sections with a total of 12 sections collected on each target. Matrix was applied using a Portrait 630 Acoustic Robotic Microspotter; sinapinic acid in 50% acetonitrile, 0.3% trifluoroacetic acid was used for protein imaging and dihydroxybenzoic acid in 50% methanol, 0.3% trifluoroacetic acid was used for peptide analysis. Each spot was approximately 180 μm with a center-to-center spacing of 200 μm (matching the spacing between sections) over the same rectangular area at the base of the brain section. Protein imaging was conducted on a Bruker Autoflex II MALDI TOF mass spectrometer resulting in 928 total peaks. Peptide imaging was carried out on a Bruker Ultraflex II MALDI TOF/TOF mass spectrometer and a total of 1,420 monoisotopic peaks were detected. Following mass spectral anlaysis, the matrix was removed from the protein data sections and the sections were stained with Cresyl violet. The stained sections could be more easily registered to each other through the alignment of structural features in the brain. The image of the unstained section was directly registered to the stained section on the MALDI plate. Amira software (Visage Imaging, Inc.) was used for the alignment of sections to each other by rigid x,y motion and z rotation. X,y scaling was not allowed as there should be no difference in size from one section to the next within the brain. Once the optimal positioning of each section had been determined, these parameters were recorded and applied to the MALDI data.

Three dimensional MALDI volumes were constructed using Image J. In addition to allowing for the co-registration of a 3D volume, Image J (http://rsbweb.nih.gov/ij/) allows for opacity mapping corresponding to the peak intensity within the mass spectral data set. In this way, relative intensities can be viewed throughout the volume in addition to their localization within the brain structures. Two z-stacks were created for the brain region, one for the protein data and one for the peptide. After successful registration and examination of these sets, they were combined to allow for visualization of colocalization or differential localization between proteins and peptides. As an example the 3D plotting of Substance P (*m/z* 1347.8) and PEP-19 (*m/z* 6717) showed that the two species colocalized throughout the substantia nigra (Figure 4). Substance P was observed in the interperduncular nucleus while PEP-19 was not. Once the volumes have been created they could be rotated up to 90° in any direction to allow for viewing from any angle without distortion of the data.

In 2008, Sinha *et al.*[27] demonstrated the ability to co-register multiple imaging modalities into the same three dimensional space. In this study, a human glioma cell line xenograft was created in the brain of an athymic nude mouse and allowed to develop. The mouse was anesthetized and subjected to high resolution longitudinal relaxation time (T_1), transverse relaxation time (T_2), and apparent diffusion coefficient (ADC) magnetic resonance imaging on a 7T magnet. Subsequent to *in vivo* imaging, the animals were sacrificed and the heads immediately snap frozen. The heads were embedded into ice blocks to allow for rigid sectioning on a cryomacrotome. Freezing and section of the entire head prevents possible distortion of the brain during the sampling process. Since the brain is entirely encased in rigid bone, reconstruction and co-registration is rendered much easier as there will be minimal to no deformation between the imaging modalities.

The heads were sectioned at 20 μm thickness with photographic images acquired of each section blockface using a Canon digital camera. A total of 20 coronal sections were collected 160 μm apart throughout the tumor bearing region of the brain. Matrix was applied to the tissue sections and protein mass spectral images were acquired on a Bruker Autoflex II MALDI TOF mass spectrometer. Image files were converted to Analyze format and

preprocessed using MATLAB and ProTSData (Biodesix, Inc.) software. This consisted of baseline correction, smoothing, and normalization to total ion current. In order to co-register all data sets in three dimensional space, first the blockface volume of digital images was reconstructed. The magnetic resonance volume was then co-registered to this volume using a 6 degree-of-freedom rigid-body normalized mutual information based registration. Because of the rigid nature of the collection of sections for mass spectrometry, they are inherently registered to the blockface volume as well and can be inserted into the image space created from the blockface and MRI. Once constructed and co-registered, these volumes can be viewed from any angle, not just the coronal orientation in which the sections were collected.

Three dimensional ion images were generated for two proteins associated with the tumor, astrocytic phosphoprotein Pea15 (*m/z* 15,035) and fatty acid binding protein 5 (*m/z* 15,076). When compared to the magnetic resonance imaging, these two proteins localized to the observed tumor area. Regions of interest were extracted from MALDI and MR images to determine correlations. There was a 233% increase in MALDI total ion current (total summed intensity of all spectral signals) in tumor as compared to normal areas of the brain. T_1 measurements were found to be slightly increased in the tumor while T_2 and ADC measurements were both found to be significantly decreased in tumor as compared to normal brain tissue. One complication in this experiment was the substantial amount of blood observed at the site of tumor cell injection into the brain. The presence of blood can complicate magnetic resonance measurements and cause ion suppression in mass spectral measurements. Nevertheless, the results of this experiment are promising in showing a correlation between non-invasive *in vivo* measurements and the biological changes occurring as observed in the post mortem mass spectral measurements.

In 2009, Chen *et al*.[28] reported the 3D mapping of lipids and peptides within the brain of a crab. In this study, brains were harvested from *Cancer borealis* and embedded in gelatin prior to snap freezing. The gelatin helped to reduce section distortion allowing for more facile section handling without producing significant background (as compared to OCT) in the mass spectral signal. A total of seven sections were collected through the z-axis of the brain at a spacing of 132 μm. Matrix (DHB) was applied to the surface of the section through the use of an airbrush. A ‘dry’ matrix application was used for lipid imaging while a commonly used wet matrix application was used for peptide analysis. Images were collected using an Applied Biosystems 4800 MALDI TOF/TOF mass spectrometer at a lateral resolution of 100 μm. Additionally, MS/MS analyses were carried out from coated and manually spotted tissue sections where individual masses for observed peptides and lipids were isolated and fragmented in the mass spectrometer whereby each unique fragment pattern could be used for identification. A total of 28 neuropeptides could be identified from manually spotted tissue sections and 20 of these peptides were observed in the coated sections for the 3D imaging experiment. Images of various peptides and lipids were viewed independently and then reconstructed into 3D volumes using Image J for viewing of the 3D projections. Although it was previously hypothesized that neuropeptides of the same class had similar distributions through the brain, these experiments showed that while this was true for some of the neuropeptides, it was not always the case. For example, the peptide NFDEIDRTGFGFH which is a member of the orcokinin peptide family shows distinct localization and high abundance in the median protocerebrum region of the brain whereas the rest of the orcokinin peptides are most abundantly expressed in the antenna I neurophil region. Another example is in the case of two members of the RFamine class of peptides, SMPSLRLRFa and DVRTPALRLFa. These two peptide are found in the antenna I neuropil region only in section one whereas other members of the RFamine class are found in the anterior medial protocerebral neuropils and the posterior medial protocerebral neuropils. In addition to the analysis of neuropeptides, mapping of lipids was also carried out in this experiment due to their importance in signal transduction and in neurological disorders and

neurodegenerative diseases. Lipids are also more diverse in neurological tissue than in any other organ system. Analyses were carried out in positive ion mode so the majority of observed species were phosphocholines (PC) and sphyngomyelins (SM). It was found that most PCs were located primarily in the main body of the brain while the SMs were more localized to the fibers, consistent with different functions in the central nervous system of the crab. In general, lipids showed less localization in the brain structures relative to that of the peptides.

3D MALDI Imaging Practical Considerations

Three-dimensional reconstruction is considerably more challenging relative to two-dimensional imaging because sectioning artifacts such as tears, folds, and deformations become more critical. All prior three-dimensional and co-registration studies have been carried out in the brain or head allowing for more facile registration and reconstruction due to encasement in the rigid skull. Recently, we have begun to explore several applications of this technology including analyses of a tumor xenograft in the hind limb of a mouse*, examining the protein distribution throughout an entire mouse pup†, and studies of a bacterial infection model in mouse kidneys. Such studies present new challenges for 3D reconstruction and co-registration due to greater risk of movement of the animal between imaging modalities and therefore additional sample preparation technique must be considered. Another interesting application of 3D IMS is in the study of metabolic exchange between microorganisms (*P. Dorrestein, unpublished symposium presentation*).‡ These organisms use chemical signals to communicate and to defend themselves when in the presence of other organisms.[29] An example is shown in Figure 5 of a 3D volume of a molecule involved in the metabolic exchange between a bacterium and a fungus.

All of the requirements for sample handling and preparation for 2D IMS also apply to 3D IMS, however, there are several additional factors to consider. An important consideration prior to the start of the IMS experiment is whether or not the IMS data will be coregistered to another 3D imaging modality such as MRI. If this is to be accomplished, the animal must not change position between the collection of the two datasets otherwise coregistration will be problematic. This is fairly easy to accomplish when working in the brain as the skull keeps all structures rigidly in place. If another anatomical feature is to be imaged, the area must be rigidly splinted during MR acquisition, sacrifice, and freezing.

The ability to reproducibly collect sections without folding or tearing is of the utmost importance for later reconstruction into a 3D volume. Although this is a practiced skill, use of semi-automated sectioning on a programmable cryostat is of great help. Recently, the introduction of the Tape Transfer System (Instrumedics, Inc.) has allowed for more rigid sample collection and transfer to a MALDI target or histology slide. In this process, a piece of transfer tape is placed on the surface of the tissue and a section is then transferred through the aid of a photoactive polymer coating on the target. The sections produced using this approach are free from tears, folds or macro distortions allowing for much easier alignment to each other and for reconstruction. Of note is that the sections of larger tissues (such as whole animals) often contain small cracks due to the bending of the tape away from the blade during sectioning. However, these cracks are often smaller than the imaging resolution of the experiment and so do not significantly interfere with image construction.

*Seeley EH, Sterling JA, Gillman AR, Sinha TK, Johnson RW, Yankeelov TE, Gore JC, Mundy GR, Matrisian LM, Caprioli RM, 58th ASMS Conference on Mass Spectrometry and Applied Topics, May 23–27, 2010, Salt Lake City, UT.
†Seeley EH, Sinha TK, Yang Z, Caprioli RM, 57th ASMS Conference on Mass Spectrometry and Applied Topics, May 31-June 4, 2009, Philadelphia, PA
‡Watrous J, Alexandrov T, Dorrestein P, 59th ASMS Conference on Mass Spectrometry and Applied Topics, June 5–9, 2011, Denver, CO

Another consideration while sectioning is the final desired voxel resolution of the image. It is often desirable to match the x,y imaging resolution with the spacing in the z-stack. If the individual tissue sections are to be microspotted at 200 μm spatial resolution, then it is prudent to collect sections 200 μm apart within the tissue block for mass spectral analysis. Sections in between the IMS sections can be collected for other purposes such as histological or immunohistochemical staining or for repeated analysis. Throughout the sectioning process, it is recommended that digital images be acquired of the sample blockface. This helps with the data registration within the animal and is essential as an intermediary if the IMS data are to be co-registered to another imaging modality such as MRI.

After collection, sections should be desiccated for a minimum of 3 hours prior to ethanol fixation for protein or peptide analysis to reduce sample loss. This fixation process helps to remove lipids, biological salts, and excess polymer that may suppress ionization of larger biomolecules.[30] Ethanol fixed or unwashed sections (for lipid or small molecule analysis) can then be stored in an air tight container at −80°C until ready for analysis.

In order to assure reproducibility between sections, it is essential that the same protocols are used to analyze all of the sections, for example, the same matrix concentration and solvent composition for sample preparation. It is recommended that a robotic spotter or nebulizer be used for matrix application (for MALDI IMS) to reduce the variability of this step. Mass spectral data should all be acquired on the same instrument using the same data acquisition method and parameters. Moreover, the data should be collected in as short a time period as is practical to minimize variations in instrument performance. Additionally, the high duty cycle required on the mass spectrometer can lead to dirtying of the source requiring cleaning and thereby affecting sensitivity. This variation can be somewhat corrected for through normalization but remains an area where technological advancements are needed. Our currently used workflow for 3D IMS and co-registration to other imaging modalities is summarized in Figure 6.

Reconstruction and co-registration is carried out using various software scripts including Amira, MATLAB, Image J, or custom software after conversion of the data to a common file structure. Scanned images of the tissue section before and after matrix spotting help with size determination and facilitate aligning to the blockface image. Once the co-registration has been completed, the data can be viewed as individual frames or slices or can be compiled into a movie.

While all steps in the 3D imaging process are critical, technological advances exist such as the Tape Transfer system, matrix application robots, and automated mass spectral acquisition software that make these processes highly reproducible. Currently, the most difficult and labor intensive step in the multi-modality imaging process is the reconstruction of the three-dimensional volume and co-registration to other image types. These processes are still largely carried out manually and are time consuming. Anticipated advances in software that can automate these processes will be significant in rapidly generating high quality multi-modality image data.

Conclusions

Imaging mass spectrometry provides a wealth of molecular information from biological specimens, providing insights that cannot easily be attained in other ways. The advent of 3D IMS has enabled a more complete picture of interactions taking place in signaling pathways and disease processes. Coupling this technology with co-registration to other imaging modalities has shown potential in bridging the gap between non-invasive functional imaging

and the underlying biology. We believe these technologies will continue to advance and will in the near future become an important technology in the clinical diagnostic toolkit.

Acknowledgments

The authors would like to thank Nicholas Winograd for data in the 3D SIMS figure. Jeramie Watrous, Theodore Alexandrov, and Pieter Dorrestein are thanked for contribution of the metabolic exchange figure. The technical assistance of Anna Crecelius and Malin Andersson in obtaining some of the unpublished data is gratefully acknowledged. The authors would also like to acknowledge funding from NIH/NIGMS 5R01 GM58008 and DoD W81XWH-05-1-0179.

Biographies

Erin H. Seeley is Research Assistant Professor of Biochemistry at Vanderbilt University. Erin received her B.S. in chemistry in 2000 from Penn State University and her Ph.D. in Analytical Chemistry in 2005 from Purdue University. She serves as Associate Director of the Tissue Profiling/Imaging Core and has worked on a wide variety of Imaging Mass Spectrometry projects. Erin's research interests are in human cancer proteomics and 3D Imaging Mass Spectrometry and its integration with other imaging modalities.

Richard M. Caprioli is Professor of Biochemistry, Chemistry, Medicine and Pharmacology at Vanderbilt University. Dr. Caprioli received his B.S. in 1965 from Columbia University in New York, N.Y., his Ph.D. in 1969 in Biochemistry, also at Columbia University. Professor Caprioli's general research interests lie in discovery of temporal and spatial processes in biological systems using mass spectrometry. Recent work involves the development of Imaging Mass Spectrometry, a technology whereby molecular images of peptides, proteins, drugs and other compounds are localized in tissue sections with molecular weight specificity.

References

1. Seeley EH, Caprioli RM. Proc Natl Acad Sci U S A. 2008; 105:18126. [PubMed: 18776051]
2. Schwartz SA, Caprioli RM. Methods Mol Biol. 2010; 656:3. [PubMed: 20680582]
3. McDonnell LA, Heeren RMA. Mass Spectrom Rev. 2007; 26:606. [PubMed: 17471576]
4. Vickerman JC. Analyst. 2011; 136:2199. [PubMed: 21461433]
5. Seeley EH, Schwamborn K, Caprioli RM. J Biol Chem. 2011; 286:25459. [PubMed: 21632549]
6. Ye H, Greer T, Li L. Bioanalysis. 2011; 3:313. [PubMed: 21320052]
7. Eberlin LS, Ifa DR, Wu C, Cooks RG. Angew Chem Int Ed Engl. 2010; 49:873. [PubMed: 20041465]
8. Nemes P, Barton AA, Vertes A. Anal Chem. 2009; 81:6668. [PubMed: 19572562]
9. Altelaar AFM, Luxembourg Stefan L, McDonnell Liam A, Piersma Sander R, Heeren Ron MA. Nat Protoc. 2007; 2:1185. [PubMed: 17546014]
10. Pacholski ML, Winograd N. Chem Rev. 1999; 99:2977. [PubMed: 11749508]
11. Lu C, Wucher A, Winograd N. Anal Chem. 2011; 83:351. [PubMed: 21121691]
12. Fletcher JS, Vickerman JC, Winograd N. Curr Opin Chem Biol. 2011
13. Fletcher JS, Rabbani S, Henderson A, Lockyer NP, Vickerman JC. Rapid Commun Mass Spectrom. 2011; 25:925. [PubMed: 21416529]
14. Chaurand P, Sanders ME, Jensen RA, Caprioli RM. Am J Pathol. 2004; 165:1057. [PubMed: 15466373]
15. Chaurand P, Schwartz SA, Reyzer ML, Caprioli RM. Toxicol Pathol. 2005; 33:92. [PubMed: 15805060]
16. Cornett DS, Reyzer ML, Chaurand P, Caprioli RM. Nat Methods. 2007; 4:828. [PubMed: 17901873]

17. Caprioli RM, Farmer TB, Gile J. Anal Chem. 1997; 69:4751. [PubMed: 9406525]
18. Stoeckli M, Farmer TB, Caprioli RM. J Am Soc Mass Spectrom. 1999; 10:67. [PubMed: 9888186]
19. Schafer R. LCGC North America. 2009:14.
20. Spraggins JM, Caprioli RM. J Am Soc Mass Spectrom. 2011; 22:1022. [PubMed: 21953043]
21. Groseclose MR, Andersson M, Hardesty WM, Caprioli RM. J Mass Spectrom. 2007; 42:254. [PubMed: 17230433]
22. Ifa DR, Wiseman JM, Song Q, Cooks RG. Int J Mass Spectrom. 2007; 259:8.
23. Reyzer ML, Hsieh Y, Ng K, Korfmacher WA, Caprioli RM. J Mass Spectrom. 2003; 38:1081. [PubMed: 14595858]
24. Wang HY, Jackson SN, McEuen J, Woods AS. Anal Chem. 2005; 77:6682. [PubMed: 16223256]
25. Crecelius AC, Cornett DS, Caprioli RM, Williams B, Dawant BM, Bodenheimer B. J Am Soc Mass Spectrom. 2005; 16:1093. [PubMed: 15923124]
26. Andersson M, Groseclose MR, Deutch AY, Caprioli RM. Nature Met. 2008; 5:101.
27. Sinha TK, Khatib-Shahidi S, Yankeelov TE, Mapara K, Ehtesham M, Cornett DS, Dawant BM, Caprioli RM, Gore JC. Nature Met. 2008; 5:57.
28. Chen R, Hui L, Sturm RM, Li L. J Am Soc Mass Spectrom. 2009; 20:1068. [PubMed: 19264504]
29. Yang YL, Xu Y, Straight P, Dorrestein PC. Nat Chem Biol. 2009; 5:885. [PubMed: 19915536]
30. Seeley EH, Oppenheimer SR, Mi D, Chaurand P, Caprioli RM. J Am Soc Mass Spectrom. 2008; 19:1069. [PubMed: 18472274]

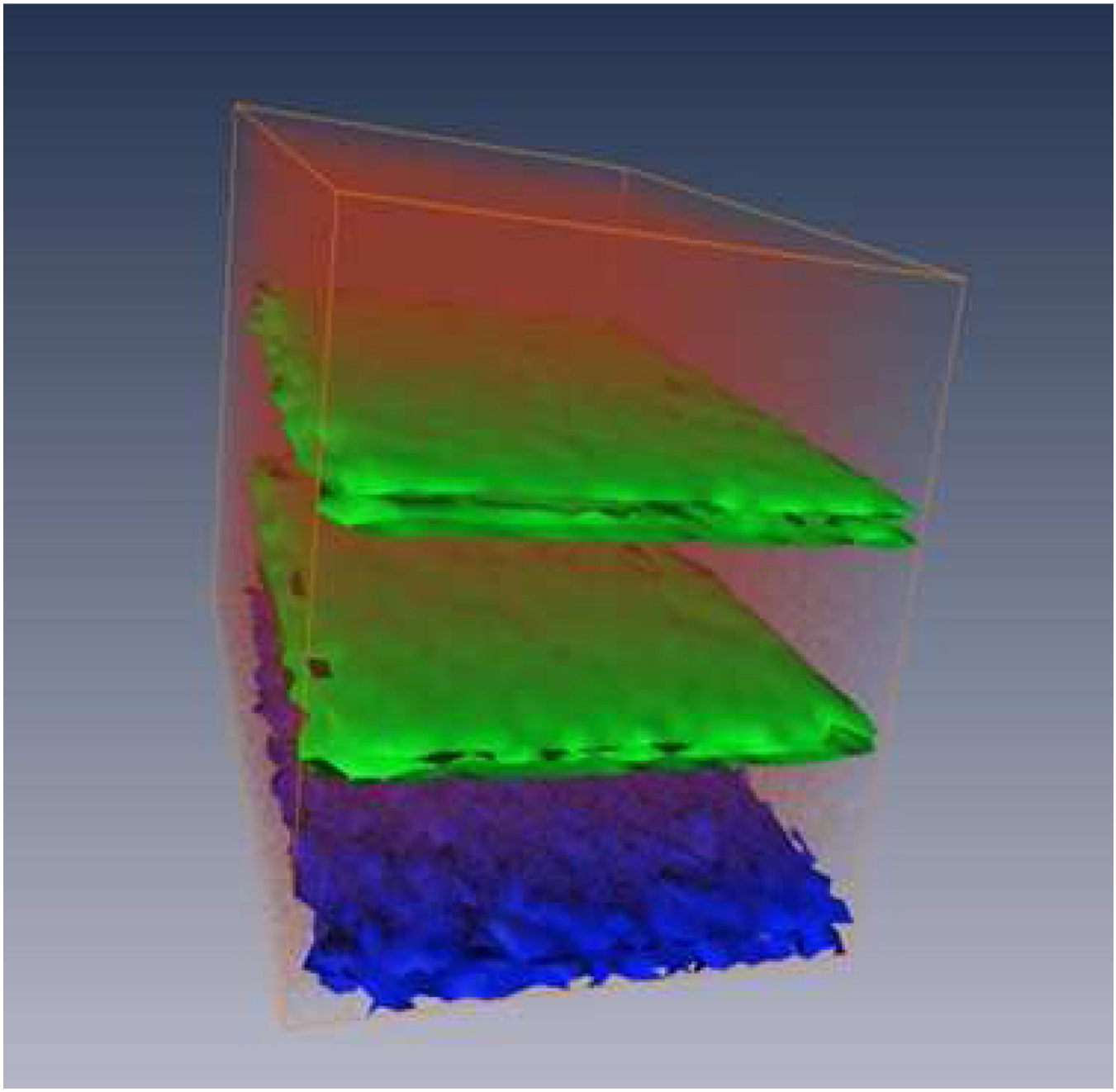

Figure 1.
Stacked images of SIMS depth profiling of Langmuir-Blodgett monolayers. The green ion corresponds to thick (51–105 nm) monolayers of barium arachidate (*m/z* 463) while the blue ion is a thin monolayer (4.4 nm) of barium dimyristoyl phosphatide (*m/z* 355). Each image layer is approximately 12.1 nm thick. *Data courtesy of Nicholas Winograd*.

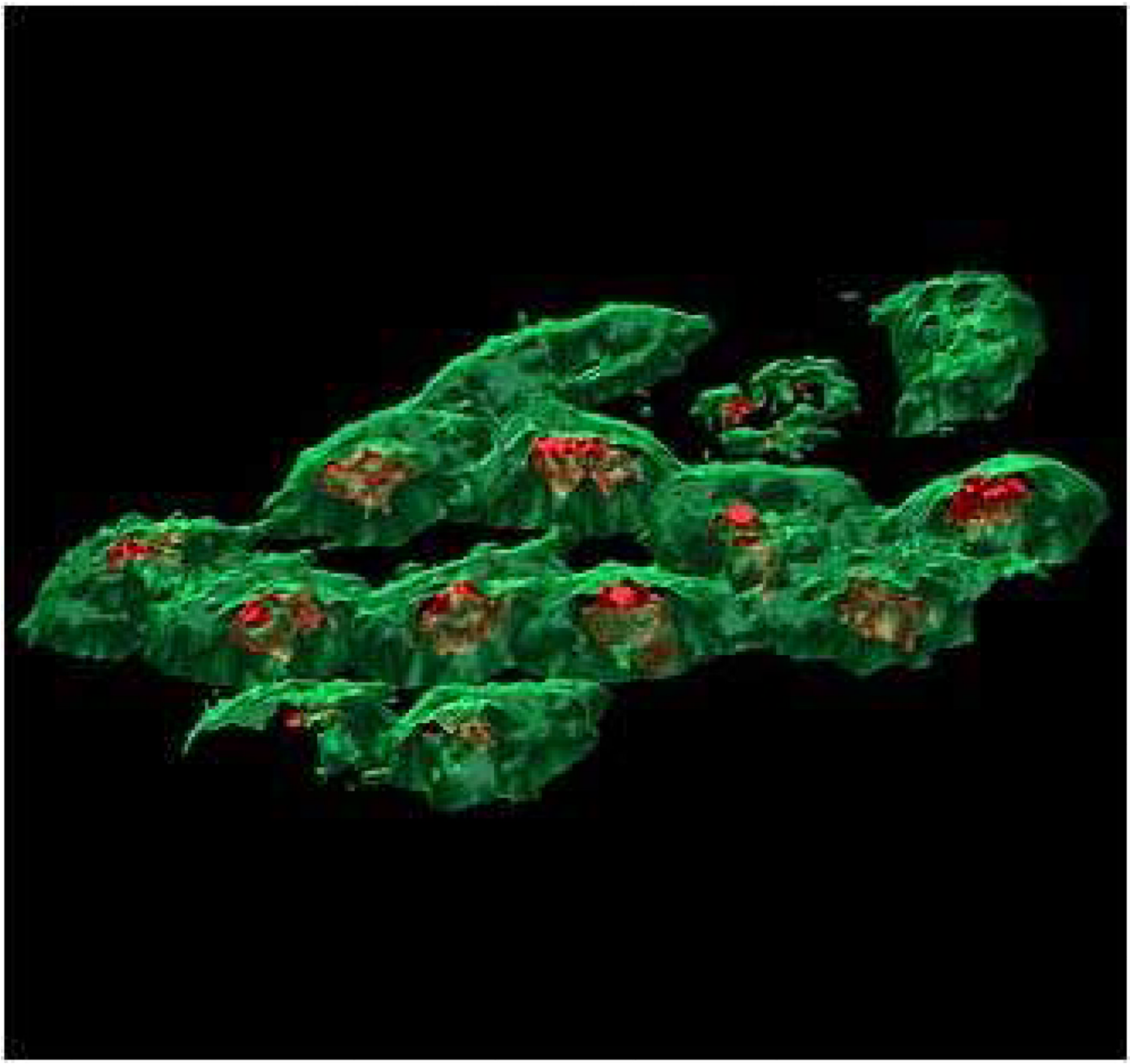

Figure 2.
3D reconstruction of SIMS depth profiling of HeLa-M cells. Phosphocholine (*m/z* 184.1) localized to the membrane is shown in green and adenine (*m/z* 136.1) localized to the nucleus is shown in red. The entire imaged area is 250 μm×250 μm. *Reprinted with permission*.[13]

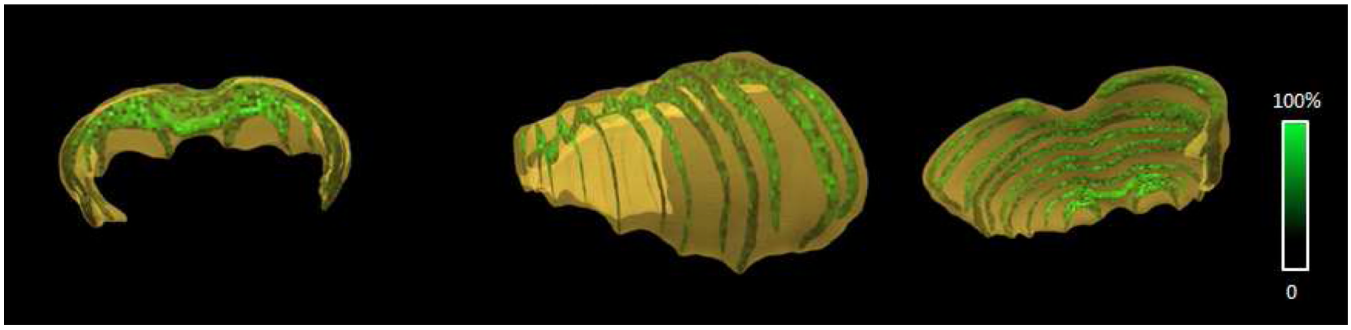

Figure 3.
Three different views of the extracted 3D volume of myelin basic protein isoform 5 (*m/z* 18415) in the corpus collosum of a mouse brain. The brown volume corresponds to the outline of the entire mouse brain.

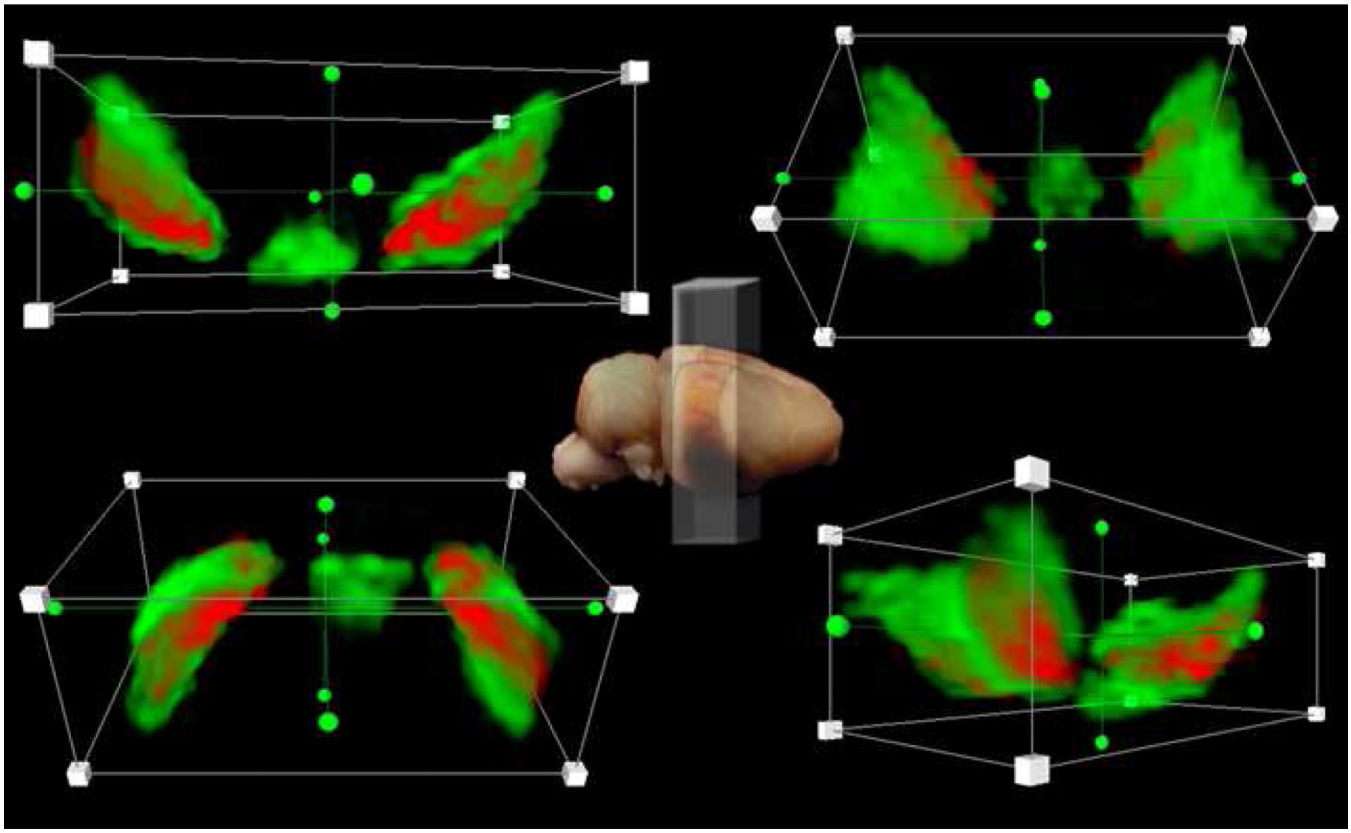

Figure 4.
Four different views of the 3D construction of the substantia nigra and interperduncular nucleus. PEP-19 is shown in green and a protein with *m/z* 7416 is shown in red. The brightest colors correspond to highest intensity.

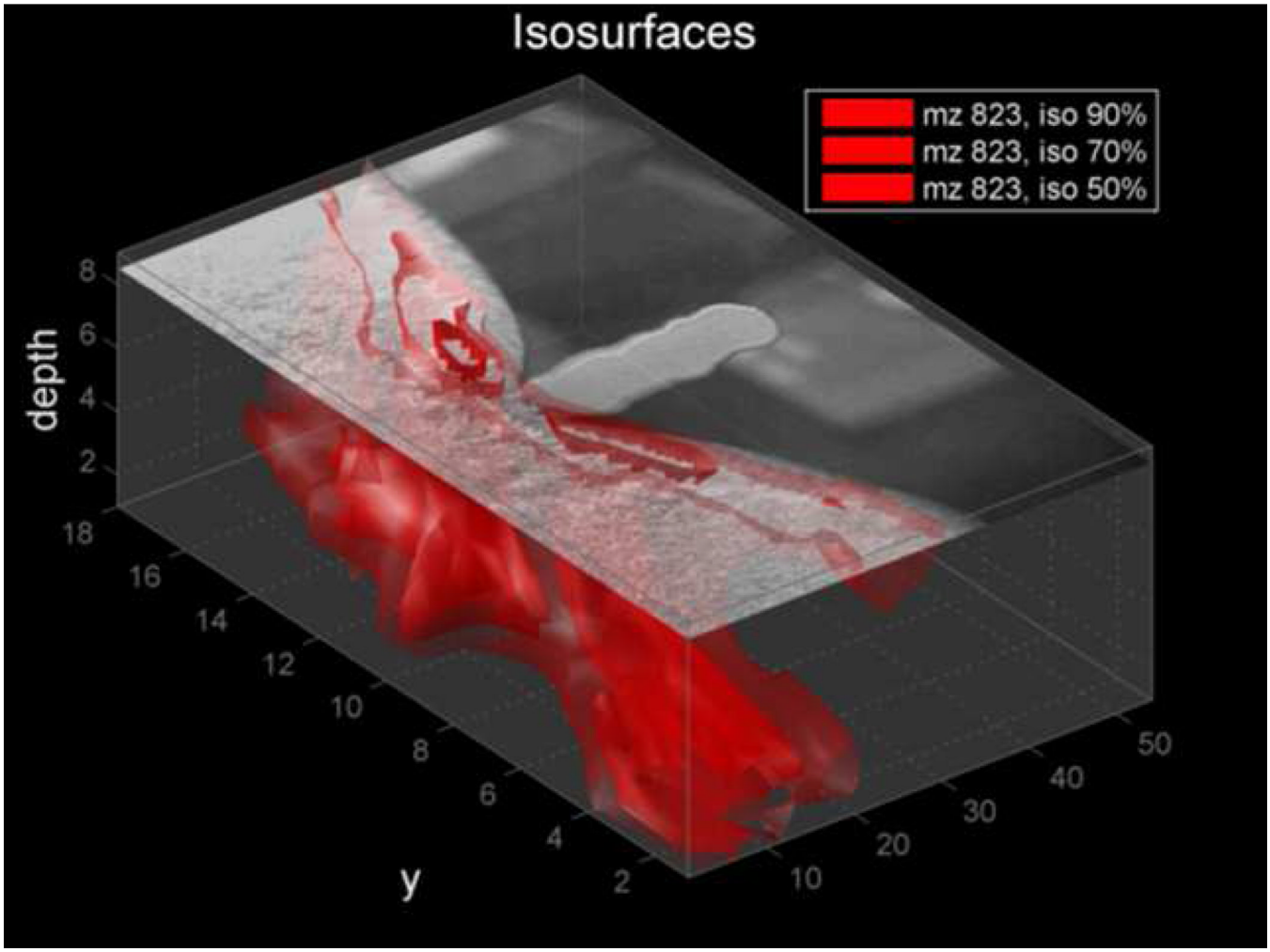

Figure 5.
3D image of a molecule involved in metabolic exchange of a fungal (left)-bacterial (right) interaction. *Data courtesy of Jeramie Watrous (Dorrestein Laboratory) and Theodore Alexandrov (Dorrestein Laboratory and University of Bremen)*.

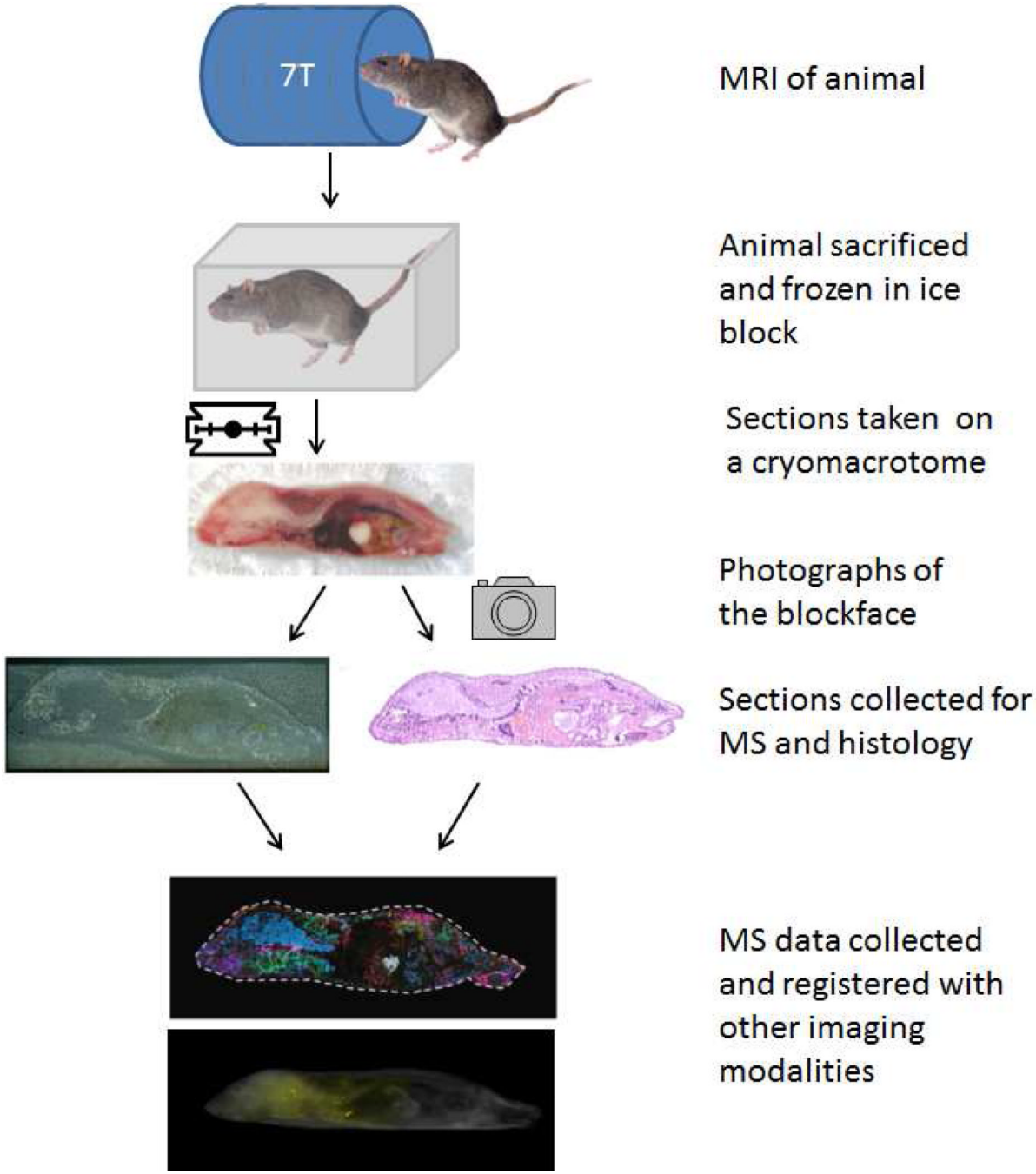

Figure 6.
Workflow for 3D IMS and co-registration. The animal is first subjected to *in vivo* imaging followed by sacrifice and freezing in an ice block. Sections are taken of the animal and IMS as well as histology images are generated. Data from multiple imaging modalities are then co-registered in the same three dimensional space.